Isothermal Crystallization of Poly(vinyl alcohol–*co*–ethylene)

Vera A. Alvarez,[1] José M. Kenny,[2] Analía Vázquez[1]

[1]*Research Institute of Material Science and Technology (INTEMA), Mar del Plata University, Juan B. Justo 4302 (7600), Mar del Plata, Argentina*
[2]*Materials Engineering Center, University of Perugia, Loc. Pentima Bassa 21, Terni, Italy.*

Received 5 June 2002; revised 10 October 2002; accepted 10 October 2002

ABSTRACT: Isothermal melt crystallization of poly(vinyl alcohol–*co*–ethylene) with different ethylene contents was studied in the temperature range of 140°C–160°C. A differential scanning calorimeter was used to follow the energy of the crystallization process. The results were analyzed by Avrami and Hoffman–Laurizten methods. The Avrami exponent was close to 2, indicating two-dimensional growth with a linear growth rate and crystals nucleating athermally. The equilibrium melting temperature was determined by the Hoffman–Weeks method. The rate of crystallization depended on ethylene content and temperature. © 2003 Wiley Periodicals, Inc. J Appl Polym Sci 89: 1071–1077, 2003

Key words: crystallization; differential scanning calorimetry; thermoplastic; biodegradable

INTRODUCTION

The study of crystallization phenomena is of great importance in polymer processing. The control of temperature during cooling, in the final stage of a process, usually determines the development of a specific morphology, which influences the final properties of the material. Therefore, the cooling rate is very important, and it can be adjusted to modulate the level of crystallinity and the crystal morphology of the polymer.[1] The modeling of nonisothermal crystallization requires knowledge of the isothermal phenomenon, which gives information on kinetics and morphology development at each crystallization temperature. The crystals grow slowly by cooling the melt or by isothermal crystallization at a temperature between the crystalline melting point and the glass-transition temperature.[2] The degree of crystallinity and morphology of the polymer, in turn, may affect the mechanical properties of the material.[3]

Analysis of the development of crystallinity during the processing of semicrystalline polymeric materials requires the application of a macrokinetic approach to describe the dependence of the degree of crystallinity on time and temperature.[4] The formation of a crystalline state from a polymer melt involves nucleation of the crystalline phase and growth of the crystal structure.[5]

Correspondence to: A. Vázquez (anvazque@fi.mdp.edu.ar).

Journal of Applied Polymer Science, Vol. 89, 1071–1077 (2003)

The aim of the present work was to study the effect of ethylene content on the crystallization of poly(vinyl alcohol–*co*–ethylene). The Avrami model was used to analyze the development of the volume fraction of crystalline phase with time.

Theoretical considerations

The heat evolved during crystallization yields exothermic peaks in differential scanning calorimetry (DSC), which represents the plot of rate of heat evolution, dQ/dt, versus temperature or time. The heat of crystallization at a constant temperature can be obtained by measuring the area under the thermogram peak, ΔH_t.[6] The crystallization kinetics of polymeric materials under isothermal conditions for various modes of nucleation and growth can be approximated by the well-known Avrami equation.[3] The general form of the Avrami expression is given as:

$$\alpha = 1 - \exp(-k \cdot t^n) \tag{1}$$

where α is the extent of crystallization [crystal conversion, calculated as $\Delta H_t/\Delta H_\infty$, the ratio of the exothermic peak areas at time t and infinite time (when crystallization is finished)], n is the Avrami exponent, and k is a rate constant, which usually follows the Arrhenius relationship with temperature:

$$k = k_0 \exp\left(-\frac{E}{R(T_m^0 - T_c)}\right) \tag{2}$$

where k_0 is a preexponential factor and E is the activation energy. The value of the Avrami exponent, n,

depends on the mechanism of nucleation and the geometry of crystal growth, and the constant, k, includes nucleation parameters as well as growth-rate parameters.

Using a theoretical approach, it can be shown that the linear growth rate, G, can be considered proportional to $1/t_{1/2}$ (crystallization half-time) based on the Hoffman–Laurizten theory.[7] The temperature variation of $1/t_{1/2}$ can be written as:

$$\frac{1}{t_{1/2}} = \frac{1}{(t_{1/2})_0} \exp\left(\frac{U}{R(T_c - T_\infty)}\right)\exp\left(\frac{K_g}{T_c f \Delta T}\right) \quad (3)$$

or, in terms of k = $1/t_{1/2}$,

$$k = k_0 \exp\left(-\frac{U}{R(T_c - T_\infty)}\right)\exp\left(-\frac{K_g}{T_c f \Delta T}\right) \quad (4)$$

where the first exponential controls the rate variations ocurring at a high degree of undercooling, when the overall crystallization is dominated by chain mobility, which decreases when the temperatures approaches the material glass-transition temperature, T_g; U is the activation energy for molecular motion, $T_\infty = T_g - 30$ K; and R is the universal gas constant. For temperatures close to T_∞, the exponential goes to zero because the mobility of the chains is remarkably reduced. The second exponential accounts for the driving force of crystallization and contains thermodynamic characteristics, such as heat of fusion, side and fold surface free energy, and the infinite-crystal melting point, T_m^0[1]; T_m^0 was determined by the Hoffman–Weeks method, extrapolating the experimental points of a plot of T_m as a function of the crystallization temperature, T_c, to the intercept with the plot $T_m = T_c$[8]; $\Delta T = T_m^0 - T_c$ is the driving force for crystallization and indicates that when temperature approaches the thermodynamic melting point, there is a substantial decrease in the overall rate of crystallization; $f = 2T_c/(T_c + T_m^0)$ is a correction term introduced to account for changes in the heat of fusion with the crystallization temperature; and K_g is a function of the surface free energy of the crystals and the heat of crystallization. The induction time, t_i, may be considered the most suitable macroscopic parameter representative of the nucleation process in calorimetric experiments. A previously proposed[4] equation for the temperature dependence of the induction time (t_i) was adopted in this study:

$$t_i = K_{ti} \exp\left\{\frac{E_{ti}}{R(T_m^0 - T_c)}\right\} \quad (5)$$

where K_{ti} is a preexponential factor and E_{ti} is the activation energy.

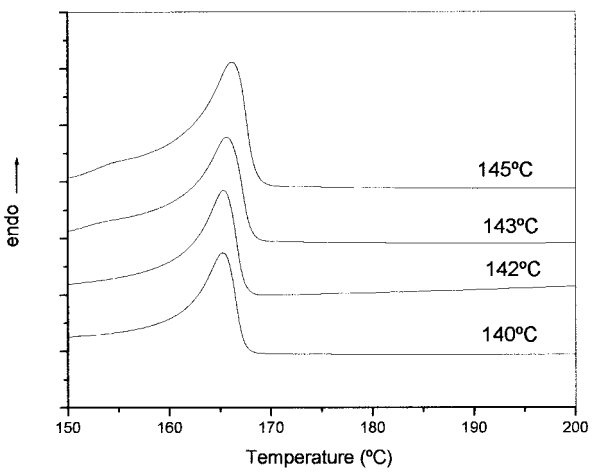

Figure 1 Dynamic DSC scan for PVOH–44% ethylene after isothermal crystallization at several temperatures.

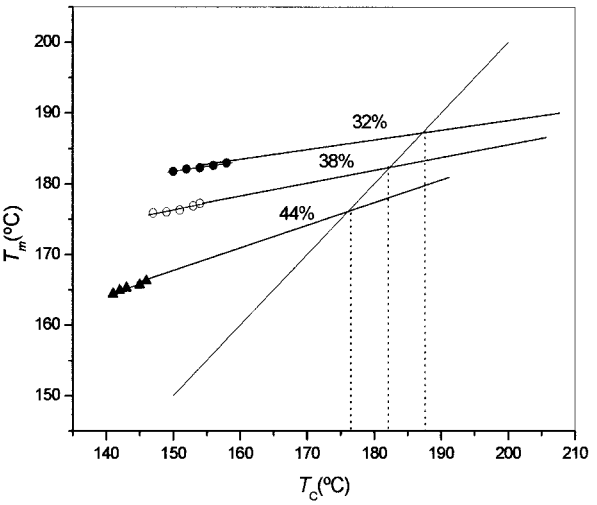

Figure 2 Hoffman–Weeks analysis. Melting point, T_m^0, as a function of the crystallization temperature, T_c, for different ethylene contents.

EXPERIMENTAL

Materials and methods

Poly(vinyl alcohol–*co*–ethylene) (PVOH–*co*–ethylene) with three molar contents of ethylene (32%, 38%, and 44%), from Sigma–Aldrich (St. Louis, MO), was used to study isothermal crystallization.

A Perkin–Elmer DSC was used for the study. A first run was done from 25°C to 250°C at 10°C/min. Then

TABLE I
T_m^0 and T_g Values for PVOH with Different Ethylene Contents

Ethylene (%)	T_m^0(°C)	T_g (°C)	Correlation coefficient
32	187.0	69	0.996
38	182.6	65	0.994
44	176.3	55	0.995

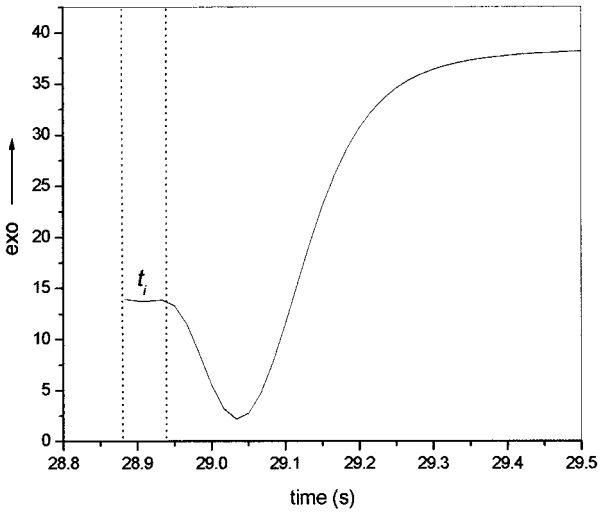

Figure 3 Crystallization exothermic peak of DSC scan for PVOH–44% ethylene crystallized at 143°C showing the induction time calculation.

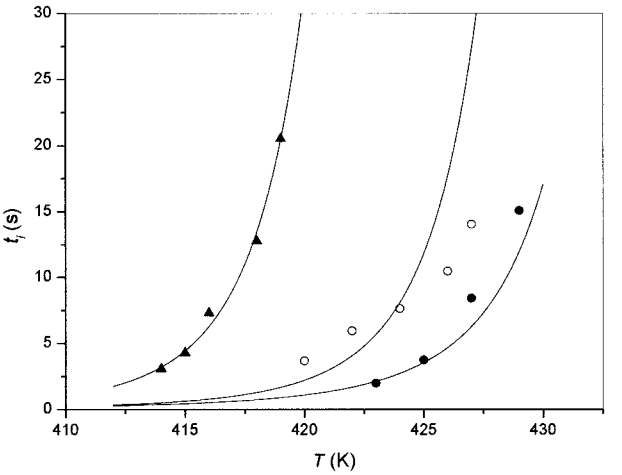

Figure 4 Induction time as a function of crystallization temperature for different ethylene contents: (●) PVOH–32% ethylene, (○) PVOH–38% ethylene, (▲) PVOH–44% ethylene. Lines represent model predictions.

the samples were melted for 10 min at 250°C, cooled to the crystallization temperature at 250°C/min, and maintained at the crystallization temperature for 20 min to allow complete crystallization. The material was crystallized in the temperature range of 140°C–160°C. Then the materials were heated from the crystallization temperature to 250°C at 10°C/min to melt formed crystals at the crystallization temperature and to find the melting temperature of each material.

Isothermal crystallization kinetics was evaluated by calculating the relative crystallinity, α (t), at time t as the fractional area confined between the heat flow-time curve and the baseline of the isothermal calorimetric curves.

Final crystallinity was also measured by using a Philips Model PW 1830 X-ray powder diffractometer equipped with a graphite monochromator and pulse height analyzer. Nickel-filtered Cu Kα radiation was used as the source.

TABLE II
Induction Times and Activation Energies for Different Ethylene Contents

Ethylene %	T_c (°C)	t_i (s)	K_{ti} (s)	E_{ti} (kJ/mol)
	150	1.32		
	152	3.72		
32	154	8.41	2.96×10^{-4}	2.75
	156	15.06		
	147	3.00		
	149	6.01		
38	151	7.62	7.40×10^{-5}	3.00
	153	9.96		
	154	14.01		
	141	3.06		
	142	4.26		
44	143	7.30	4.12×10^{-5}	3.30
	145	12.75		
	146	20.52		

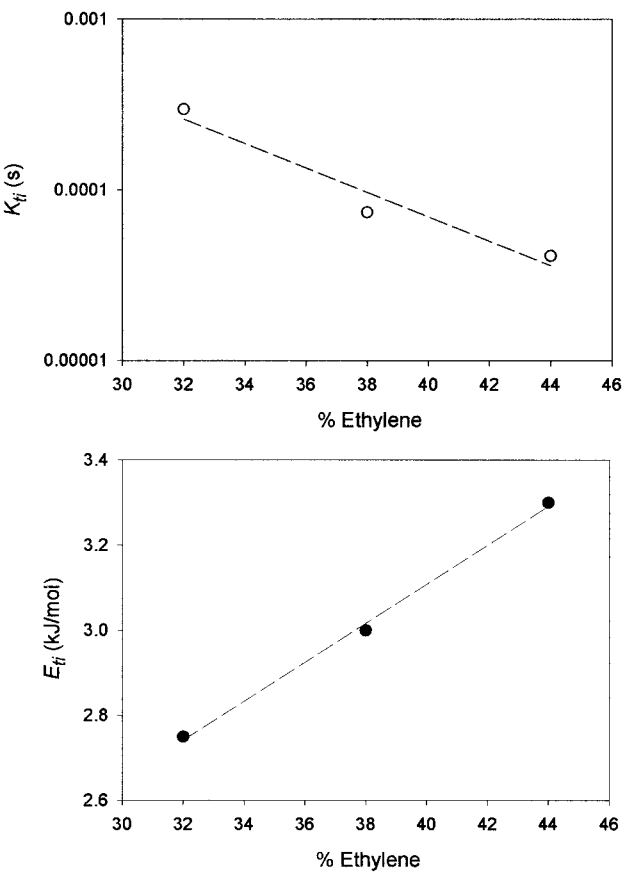

Figure 5 (a) Preexponential values and (b) activation energy values in function of ethylene content in poly(vinyl alcohol–*co*–ethylene) copolymer.

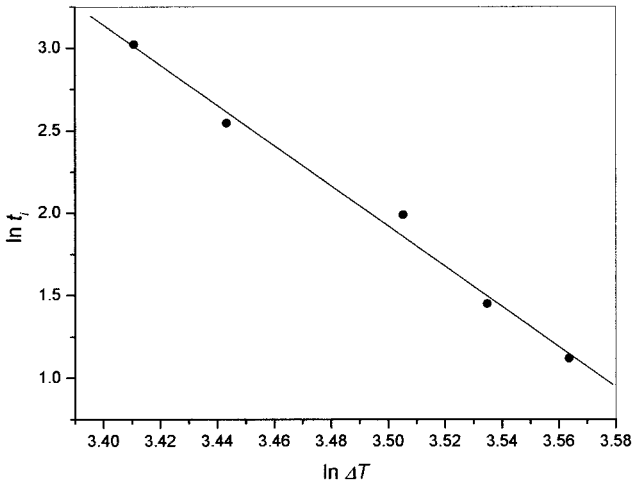

Figure 6 Induction time as a function of undercooling for PVOH–44% ethylene.

RESULTS AND DISCUSSION

Figure 1 shows the DSC results of the PVOH–44% ethylene samples after isothermal crystallization runs. It can be seen that the melting temperature increased when the isothermal crystallization temperature increased. This tendency was present in all materials and occurred because chain mobility increases when crystallization temperature increases, allowing formation of larger crystals and leading to higher melting temperatures. Because of the different crystallization conditions, different morphologies were obtained by varying the level of undercooling. A higher number of nuclei could be obtained at lower crystallization temperatures, leading to the formation of a larger number of smaller crystals.[1]

TABLE III
Experimental Data and Results of Avrami Equation Parameters for Materials Used

Ethylene %	T_c (°C)	t_i (s)	$t_{1/2}$ (s)	ln k	n	T_m (°C)
	150	1.32	4.08	−3.11	1.93	181.8
	152	3.72	6.74	−4.12	2.13	182.1
32	154	8.41	8.18	−4.43	2.36	182.3
	156	15.06	11.62	−5.16	2.27	182.6
	147	3.00	4.05	−3.30	1.87	175.9
	149	6.01	4.65	−3.86	1.89	176.1
38	151	7.62	7.06	−4.516	2.18	176.3
	153	9.96	10.88	−4.83	2.20	177.2
	154	14.01	16.40	−5.70	2.36	178.8
	141	3.06	4.00	−4.47	2.28	164.4
	142	4.26	5.70	−4.54	2.28	164.8
44	143	7.30	6.91	−5.05	2.36	165.2
	145	12.75	10.86	−5.76	2.28	165.7
	146	20.52	16.04	−5.94	2.03	166.2

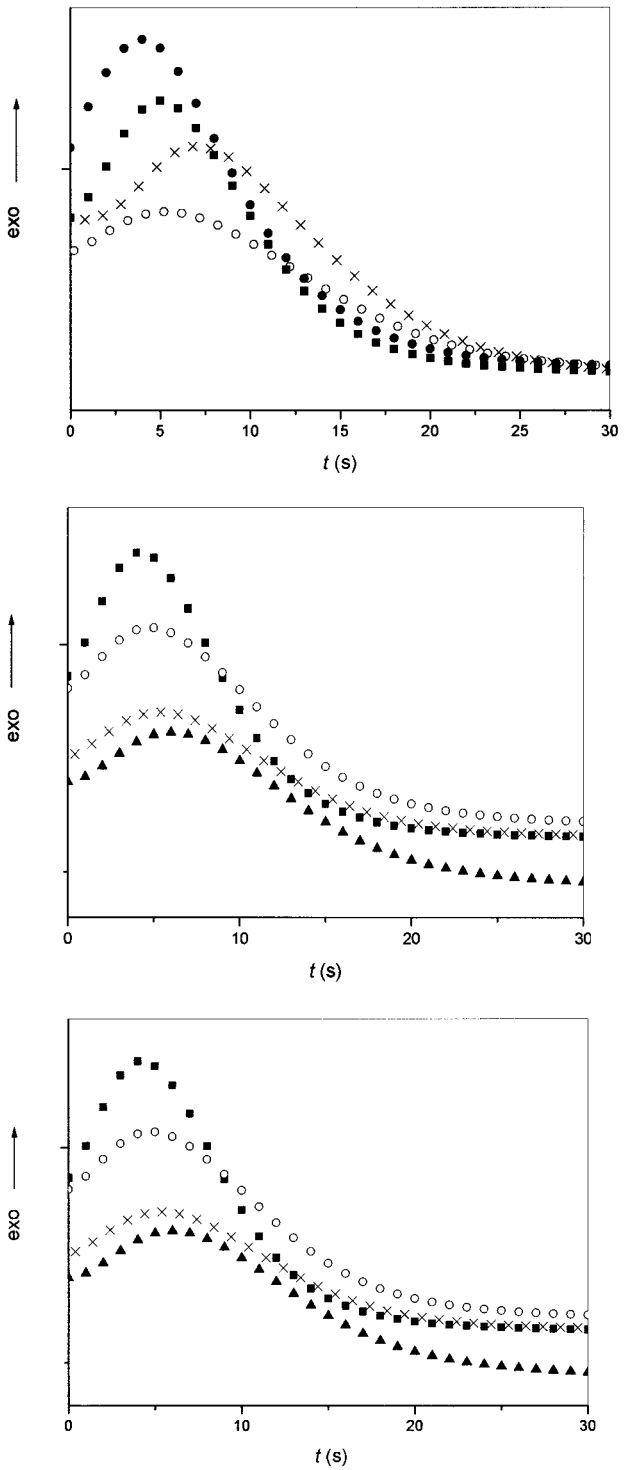

Figure 7 (a) DSC crystallization exothermic peaks for PVOH–32% ethylene at different temperatures: (●) T_C = 150°C, (■) T_C = 152°C, (×) T_C = 154°C, (○) T_C = 156°C; (b) DSC crystallization exothermic peaks for PVOH–38% ethylene at different temperatures: (■) T_C = 147°C, (○) T_C = 149°C, (×) T_C = 151°C, (▲) T_C = 153°C; (c) DSC crystallization exothermic peaks for PVOH–38% ethylene at different temperatures: (■) T_C = 141°C, (○) T_C = 143°C, (×) T_C = 145°C, (▲) T_C = 146°C.

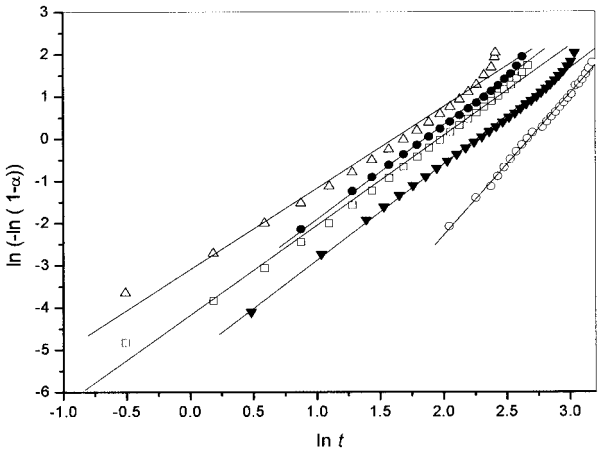

Figure 8 Avrami analysis for PVOH–32% ethylene at different crystallization temperatures: (△) Δ T_C = 141°C, (●) T_C = 142°C, (□) T_C = 143°C, (▼) T_C = 145°C, (○) T_C =146°C.

To obtain the equilibrium melting point, T_m^0, a Hoffman–Weeks plot of the DSC data was done (Fig. 2). Linear regression of crystallization data was used, and a good alignment on a straight line was confirmed by the correlation coefficients. Glass-transition temperature, T_g, reflects the mobility of polymer chains and is therefore a useful complement to our isothermal crystallization studies (performed in a temperature range at which mobility of all samples is quite high). Because the rate of crystallization is zero at the glass-transition and melting temperatures, $1/(T_m^0 - T_c)$ may be assumed as a driving force for crystallization and $1/(T_c - T_g)$ as a diffusion-controlled driving force accounting for the increase of viscosity when the temperature approaches T_g. The T_m^0 and T_g values for the materials employed are reported in Table I.

Figure 3 shows the induction time at a given T_c, defined as the time for formation of an equilibrium nucleus with critical dimensions[9] for the PVOH–44% ethylene crystallized at 143°C. Using eq. (5), by plotting ln t_i versus $1/(T_m^0 - T_c)$, we calculated K_{ti} and E_{ti} values. The experimental data are reported in Table II. It can be seen that the activation energy, E_{ti}, increased when ethylene content increased, indicating that ethylene in the copolymer chain hinders the nucleation process of PVOH–*co*–ethylene. Figure 4 shows the induction time dependence on temperature for PVOH–*co*–ethylene containing different contents of ethylene (experimental data and model predictions). It can be seen that the model is in agreement with most of the experimental data. For all ethylene contents used, induction time increased when crystallization temperature increased; this is because the undercooling, the driving force for the crystallization process, decreased. Figure 5(a,b) shows the relationship between the obtained values of, respectively, K_{ti} and E_{ti} with ethylene content. Figure 6 shows the induction time as a function of undercooling for PVOH-44% ethylene.

Growth is related to the exothermic peak shown on the DSC scan. Figure 7 shows the crystallization peaks for different ethylene contents and several crystallization temperatures. It can be seen that crystallization rate decreased when crystallization temperature increased because of less undercooling, which is the driving force for crystallization.

TABLE IV
Results of Arrhenius Equation for PVOH with Different Ethylene Contents

Ehylene (%)	k_0 (s^{-n})	E (kJ/mol)
32	687.1	3.03
38	364.2	2.72
44	200.7	2.85

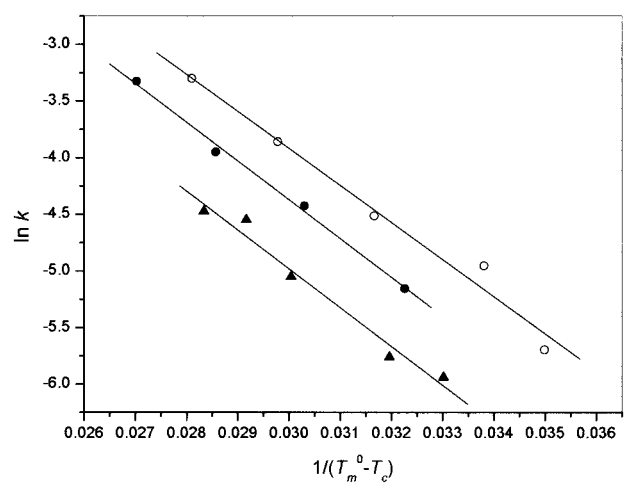

Figure 9 Plot of ln k versus $1/(T_m^0 - T_c)$ for different materials used: (●) PVOH–32% ethylene, (○) PVOH–38% ethylene, (▲) PVOH–44% ethylene.

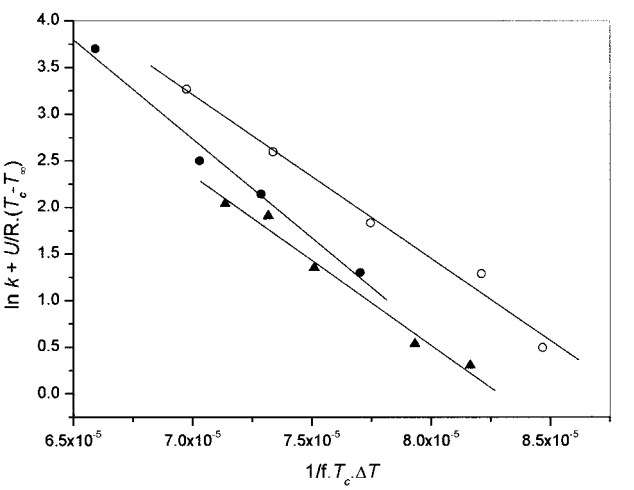

Figure 10 Plot of ln k + $U/[R(T_c - T_\infty)]$ versus $1/(f\,T_c\,\Delta T)$ for different materials: (●) PVOH–32% ethylene, (○) PVOH–38% ethylene, (▲) PVOH–44% ethylene.

TABLE V
Results of Hoffman–Laurizten Analysis for Different Ethylene Contents

Ethylene (%)	k_0 (s^{-n})	K_g (K^2)
32	4.48×10^7	1.76×10^5
38	5.53×10^6	1.82×10^5
44	3.56×10^6	2.12×10^5

Once the crystallization time is scaled by the induction time, the parameters of the Avrami model can be calculated using the classical double logarithm method on both sides of eq. (1). Figure 8 shows a linear regression of $\ln[-\ln(1 - \alpha)]$ as a function of $\ln t$. The values obtained using the Avrami equation are reported in Table III. The average of all the Avrami exponents for linear systems was close to 2, which may be interpreted as two-dimensional crystal growth, with a linear growth rate, heterogeneous nucleation,[10] and the crystal nucleating athermally.[11] Athermal nucleation implies there is no contribution from the nucleation rate to the activation energy.[5]

Using the Arrhenius equation, the rate constant can be modeled. Applying logarithms to both sides of eq. (2), the dependence of k on the degree of undercooling (ΔT) was determined. Figure 9 shows a linear regression of $\ln k$ as a function of $1/\Delta T$. From this plot it is possible to obtain the activation energies for materials used. The results of this regression are reported in Table IV. The activation energy was close to 2.88 kJ/mol for all materials. The preexponential factor (k_0) decreased when ethylene content increased, indicating that crystallization was slower for higher ethylene contents.

Using Hoffman–Laurizten analysis, following the proportionality between k and G, and applying logarithm to both sides of eq. (4), the following equation can be written:

$$\ln k + \frac{U}{r(T_c - T_\infty)} = \ln k_0 - \frac{K_g}{fT_c\Delta T} \qquad (6)$$

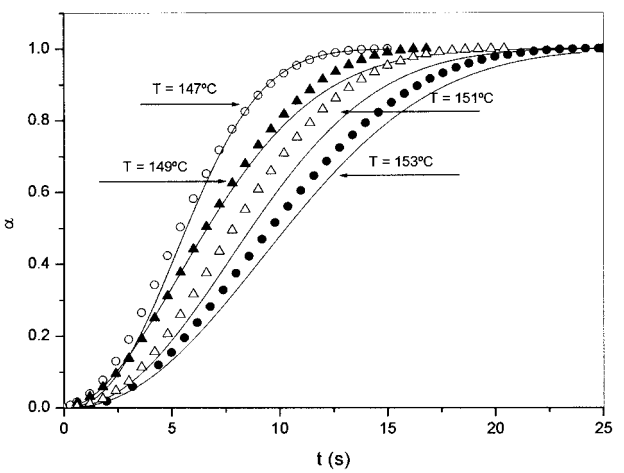

Figure 11 Degree of crystallinity as function of time for PVOH–44% ethylene. Line represents model prediction from Hoffman–Laurizten analysis.

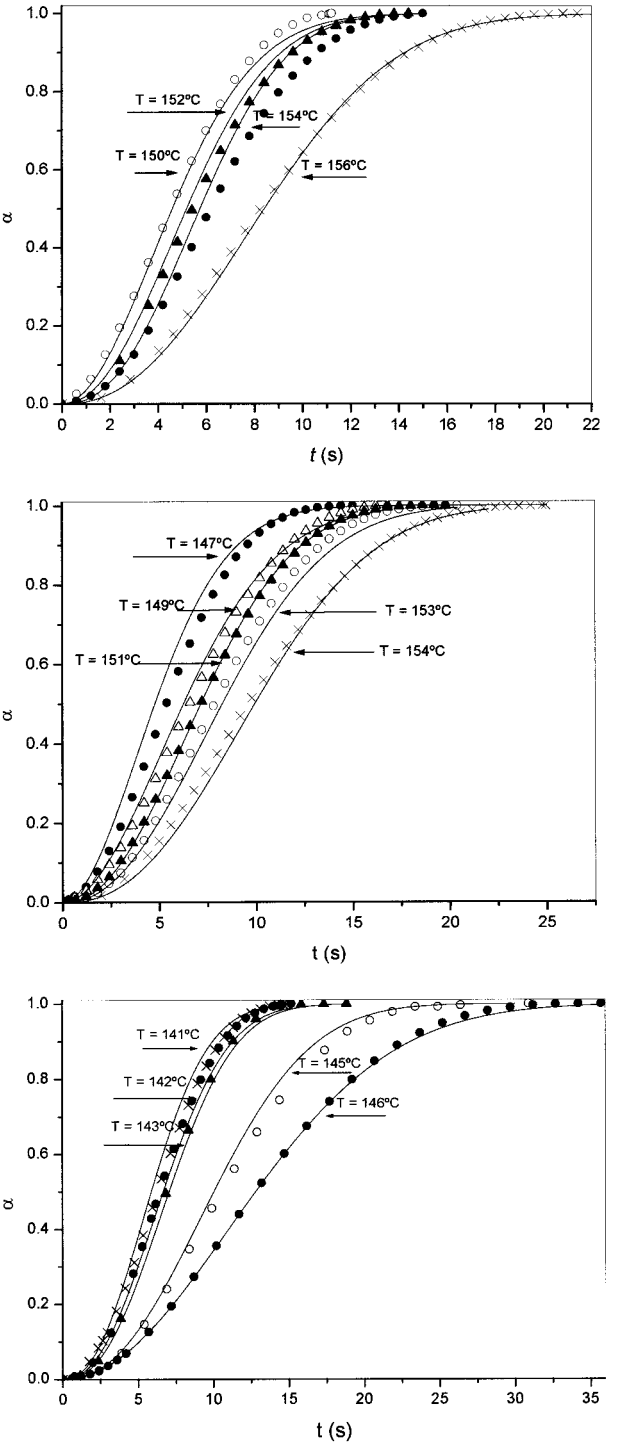

Figure 12 (a) Degree of crystallinity as a function of time for PVOH–32% ethylene, (b) degree of crystallinity as a function of time for PVOH–38% ethylene, (c) degree of crystallinity as a function of time for PVOH–44% ethylene. Line represents Avrami model prediction.

where U is 1500 cal/mol, which was used in previous studies[12] and is employed here to fit the experimental data. Figure 10 shows $\ln k + U/[R(T_c - T_\infty)]$ versus $1/(f\,T_c\,\Delta T)$. From this plot the k_0 and K_g values were calculated. These values are reported in Table V. An increase in ethylene content produced a decrease in k_0; this indicates that crystallization is slower when ethylene content increases. On the other hand, K_g increased with ethylene content, so that the value for the second exponential in eq. (6) became lower, decreasing the crystallization rate.

Figure 11 shows the experimental data for the extent of crystallization and the values obtained with the macrokinetic model derived from the Hoffman–Lauritzen model. The α values calculated with this model are in agreement with the experimental data. However, the Avrami model (Fig. 12) was in better agreement. It can be seen that when the crystallization temperature was close to the melting temperature (low undercooling), the crystallization time increased and the crystallization rate decreased.

Figure 13 shows the spectrum of poly(vinyl alcohol–*co*–ethylene) with different contents of ethylene. Table VI shows that crystallinity increased when ethylene content increased. The results shown in Tables IV and V indicate that the ethylene content in the chain of the PVOH–*co*–ethylene copolymer decreased molecular mobility, and a large activation energy was needed for the polymer chain to diffuse into the crystalline lattice, which led to lower crystallization rates. The ethylene chain produced a larger quantity of crystal which was obtained at a lower crystallization rate, indicating that it led to a more perfect crystalline structure.

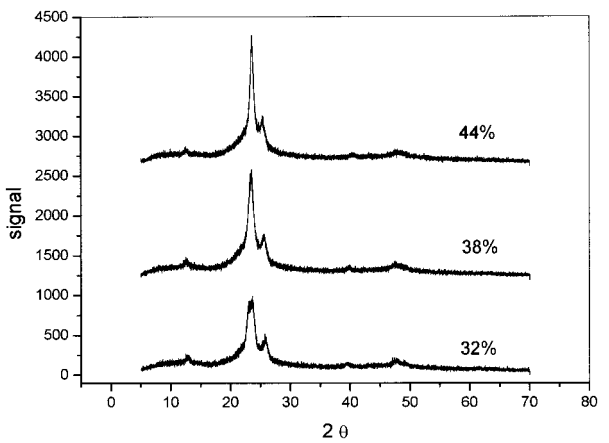

Figure 13 Spectrum of X-ray of poly(vinyl alcohol–*co*–ethylene) for different ethylene contents.

TABLE VI
Crystallinity Measured by X-ray

Ethylene	Crystallinity
32	0.48
38	0.56
44	0.60

CONCLUSIONS

The slow crystallization process of PVOH–*co*–ethylene was exploited in order to test the applicability of a previously developed kinetic model through all the crystallization ranges between T_g and T_m^0. The model provided an expression for the induction time and temperature dependence of the kinetic constant.

The temperature dependence of the rate constants for each of the processes in the crystallinity model was found to follow Arrhenius relationships. Activation energies were close to 2.88 kJ/mol for all systems, but the preexponential factors decreased when the ethylene content increased.

Isothermal crystallization kinetics of these materials was studied as a function of the degree of undercooling. The overall rate of bulk crystallization followed the Avrami equation with the exponent n close to 2, which has been interpreted as two-dimensional crystal growth with a linear growth rate and the crystals nucleating athermally.

The crystallization rate showed a maximum at the lowest crystallization temperature for all the systems studied. When PVOH–*co*–ethylene was crystallized at a high degree of undercooling, crystallization was faster. When the content of ethylene in the PVOH–*co*–ethylene copolymer increased, the final crystallinity increased, but the crystallization rate was low.

References

1. Iannace, S.; Nicolais, L. J Appl Polym Sci 1997, 64, 911.
2. Cebe, P.; Hong, S. D. Polymer 1986, 27, 1183.
3. Bogoeva-Gaceva, G.; Janevski, A.; Grozdanov, A. J Appl Polym Sci 1998, 67, 395.
4. Torre, L.; Maffezzoli, A.; Kenny, J. M. J Appl Polym Sci 1995, 56, 985.
5. Desio, G. P.; Rebenfeld, L. J Appl Polym Sci 1992, 45, 2005.
6. Lin, C. C. Polym Eng Sci 1983, 23(3), 113.
7. Hoffman, J. D.; Frolen, L. J.; Ross, G. S.; Lauritzen, J. I. J Res NBS 1975, 79A, 671.
8. Avella, M.; Martuscelli, E.; Selliti, S.; Caragnani, E. J Mater Sci 1987, 22, 3180.
9. Janevsky, A.; Bogoeva-Gaceva, G. J Appl Polym Sci 1998, 69, 381.
10. Reinsch, V. E.; Rebenfeld, L. J Appl Polym Sci 1994, 52, 649.
11. Di Lorenzo, M. L.; Silvestre, C. Prog Polym Sci 1999, 24, 917.
12. Maffezzoli, A.; Kenny, J. M.; Nicolais, L. J Mater Sci 1993, 28, 4994.